Identification of the mechanism-limiting nitrogen diffusion in metallic alloys by *in situ* photoemission electron spectroscopy

C. A. Figueroa, A. S. Ferlauto, and F. Alvarez[a)]
Instituto de Física "Gleb Wataghin," Universidade Estadual de Campinas, Unicamp 13083-970, Campinas, São Paulo, Brazil

(Received 18 April 2003; accepted 10 July 2003)

In situ photoemission electron spectroscopy is used to identify the mechanism limiting the thermally activated nitrogen diffusion in metallic alloys. The samples were prepared by bombarding stainless steel with a broad ion source in a high-vacuum chamber. The photoemission spectra evolution on increasing controlled oxygen partial pressure is correlated with bulk material properties. The presence of oxygen inhibits the formation of iron nitrides and γ_N-phase (*austenitic* face-centered-cubic lattice containing nitrogen), which proved to be fundamental for efficient nitrogen penetration in the alloy. © *2003 American Institute of Physics.*
[DOI: 10.1063/1.1605250]

An understanding of the surfaces phenomena is very important to control the diffusion processes in solids. In the diffusion process, the first step is the formation of a high concentration of species of the precursor on top and/or underneath. Subsequently, the species diffuse into the bulk by a thermally activated process. Therefore, the mechanisms determining the compounds at the surface and subsurface regions will control the diffusion process. This simple picture stresses the importance of a careful surface study to better understand the diffusion processes in solids. This is particularly important for nitrogen diffusion in metallic alloys, like stainless steel where stringent exigencies such as corrosion resistance, hardness, strength, and low resistance coefficient are required.[1,2] Plasma nitrating is an important technology currently being used to improve the properties of the alloy. Basically, this process consists first of nitrogen ion implantation and, then, bulk thermal diffusion. Unexpectedly, although this technique is widespread, the microscopic phenomenon occurring at the material surface is not well understood. Indeed, an interplay involving plasma, gaseous phases (including residual oxygen), nitrides surface formation, and sputtering, makes the problem particularly complex. The microscopic role at the material surface of oxygen on the nitrogen diffusion processes is especially important. For instance, it is well established that above a critical oxygen partial pressure, the formation of a potential barrier diminishes the nitrogen diffusion into the bulk.[3,4] Therefore, a better understanding of how the oxygen interacts with nitrogen and the metallic surface is of primordial importance for the further improvement and control of nitrogen diffusion in bulk. Finally, we stress the importance of performing the experiments *in situ*, i.e., in a very precisely controlled atmosphere to elucidate the role of oxygen.

We report the identification of the mechanism-limiting nitrogen diffusion in a metallic alloy by an *in situ* photoemission electron spectroscopy (XPS) study. The material was implanted with low-energy nitrogen ions (0.6 keV). XPS is a well-established technique proving the structure and composition of the top-most surface atomic layers.[5] In this specific study, nitrides and oxygen species, which form underneath the material surface, are the focus of interest.

Mirror polished, rectangular samples, 20×10 mm and 1 mm thick were prepared from the same commercial AISI 316 stainless-steel lot (C: <0.08, Si: <0.5, P: 0.05, S: 0.03, Mn: 1.6, Mo: 2.1, Ni: 12.0, Cr: 17.0, Fe: balance). The implantation was performed in a high-vacuum chamber, with a 3 cm diameter dc Kaufman ion source attached to an ultrahigh-vacuum chamber for XPS analysis.[6] The sample temperature was maintained at (380 ± 10)°C for the implantation time of 30 min. This time was chosen to ensure that a compositional dynamic equilibrium is reached at the sample surface. As shown next, results obtained in samples implanted for 60 min confirm the equilibrium assumption. The background chamber pressure was $<10^{-4}$ Pa ($P_{O_2}<2\times10^{-5}$ Pa). Nitrogen was introduced directly into the ion source with a constant flow rate, resulting in a partial pressure of 10^{-2} Pa. The oxygen partial pressure was varied from 10^{-3} to 10^{-2} Pa. In order to maintain a fixed total pressure (8.3×10^{-1} Pa), an appropriated hydrogen flux was added into the chamber, guaranteeing a constant N_2^+ mean-free path for all experiments.[7] Oxygen and hydrogen gases were introduced in the chamber through an independent inlet (i.e., not through the ion source). The nominal current density and energy of the N_2^+ ion beam were fixed at 5.7 mA/cm^2 and 600 eV, respectively. For N_2^+ ions having this energy, numerical simulation shows that the thickness of the implanted nitrogen layer is ~4–5 nm.[8] Conveniently, this thickness is similar to the characteristic escape depth for photoemitted electrons with kinetic energy in the 200–1500 eV energy range.[5] Immediately after nitrogen implantation, the chamber is flooded with helium, rapidly cooling the samples. Finally, the samples are transferred to the attached ultrahigh-vacuum chamber for XPS analysis. The XPS spectra were obtained by using the 1486.6 eV photons from an Al

[a)]Author to whom correspondence should be addressed; electronic mail: alvarez@ifi.unicamp.br

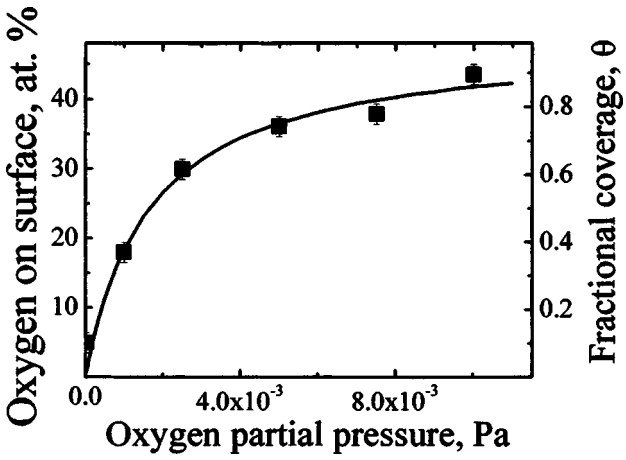

FIG. 1. Absorbed oxygen and fractional coverage vs oxygen partial pressure. The solid line represents the theoretical fitting using a Langmuir isothermal adsorption law.

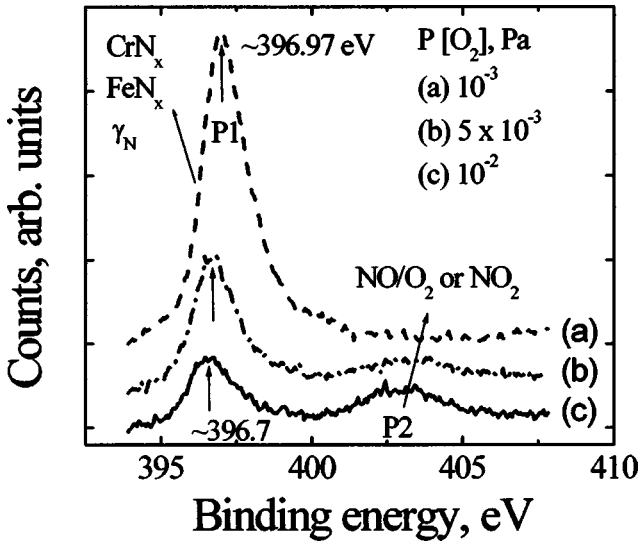

FIG. 2. N 1*s* core-level photoemission spectra of samples implanted at different oxygen partial pressures. For the sake of clarity, the spectra are vertically shifted and only a few of them are shown.

target ($K\alpha$ line) and a VG-CLAMP-2 electron analyzer. The total apparatus resolution was ~0.85 eV (linewidth plus analyzer).[6] The relative atomic composition at the surfaces of the sample was determined by integrating the core-level peaks, properly weighted by the photoemission cross section.

The depth of the nitrated layers was revealed by attacking the samples at room temperature with Marble's solution (10 g copper sulfate in 100 ml of 6 M hydrochloric acid) and measured by scanning electron microscopy [(SEM)/JEOL JMS-5900LV]. The nitrated layer thickness was directly obtained from the SEM images. The hardness was obtained using a Berkovich diamond tip (*NanoTest-300*) and load–displacement curves were analyzed using the Oliver and Pharr method.[9]

Figure 1 shows the oxygen concentration and the fractional coverage as a function of oxygen partial pressures in the chamber. The oxygen concentration was obtained from the O 1*s* energy bands of the photoemission spectra (not shown). The *fractional coverage* θ is defined as the quotient between the total available surface sites and the actually covered surfaces sites. Assuming the formation of a tiny oxidized overlayer, the experimental data are quite well represented by a Langmuir isothermal adsorption law given by (Fig. 1, solid line):[10,4]

$$\theta = \sigma/\sigma_0 = PO_2/(PO_2 + P^*). \quad (1)$$

Here, σ is the actual fraction of the surface covered by oxygen, σ_0 is the maximum available area to be covered, and PO_2 is the partial pressure of oxygen at the working condition. Finally, $K^{-1} \equiv P^*$ is the adsorption–desorption constant which is strongly dependent upon temperature. P^* represents the necessary oxygen pressure to cover 50% of the surface ($\theta = 0.5$). The fitting of the experimental data with Eq. (1) gives $\sigma_0 \sim 49\%$ and $P^* \sim 1.7 \times 10^{-3}$ Pa. The rather low P^* shows that at a very low oxygen partial pressure, oxygen atoms will cover half of the surface available sites.

Figure 2 shows the N 1*s* core electron level photoemission spectra of some of the studied samples. At a relatively low oxygen partial pressure, only one band is present at ~397 eV which is associated with FeN_x and N dissolved in the alloy as the (γ_N) phase.[11–13] Upon increasing the oxygen partial pressure, P1 shifts to a lower binding energy. This is due to the formation of other precipitates species, like CrN_x (~396.6 eV).[14] Simultaneously, a band ($P2 \sim 403.0$ eV) arises which is associated with NO/O_2 and/or NO_2. As found by Folkesson,[15] the energy position of the observed band is associated with charge transference due to the presence of two oxygen atoms bonded to nitrogen. A detailed analysis of these effects is beyond the scope of this article and will be reported in a future study.

In order to elucidate the bonding mechanism of nitrogen at the surface, a quantitative analysis of the XPS was performed. The peak P1 was deconvoluted assuming two metallic compounds, i.e., FeN_x and N in the γ_N phase, and nonferrous nitrides, mainly formed by Cr nitrides. Here, γ_N is the *austenitic* face-centered cubic [lattice containing nitrogen].[16] Figure 3 shows the dependence of these components as a function of the oxygen atomic content. At a low oxygen partial pressure, the FeN_x and γ_N species are dominant. Increasing the oxygen diminishes this compound. On the other hand, CrN_x is approximately constant upon increasing the oxygen partial pressure. Figure 4 provides information about the role of each species in the nitriding diffusion process. Figure 4 represents the hardness (at 0.4 μm depth) and total thickness of the nitrated layer versus N content in the form of FeN_x and γ_N compounds. In this analysis, there is no way to distinguish the main N diffusion precursor. However, N in the γ_N phase is probably the species responsible for efficient nitrogen diffusion in the bulk material. This is due to the great stability of the metallic compounds. The filled and empty squares of Fig. 4 represent two sets of samples implanted for 30 and 60 min, respectively. For completeness, the open circles in Fig. 4 represent the layer thickness of the 60 min deposited samples. The rather linear dependence on nitrogen content in the form of FeN_x and γ_N strongly suggests that these are the ''active sites'' for efficient nitrogen diffusion in the material bulk. Returning to

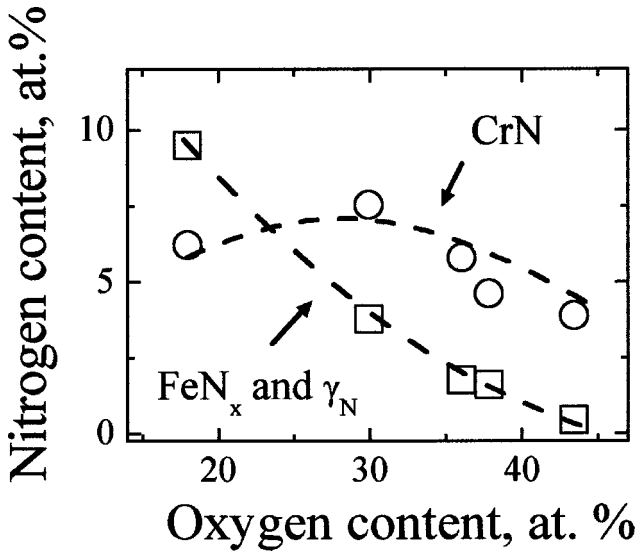

FIG. 3. Nitrogen content in different nitrides species vs oxygen content. The experimental errors are of the order of the symbol size.

Fig. 3, one can conclude that the oxygen covering the surface material diminishes the formation of the FeN_x and γ_N species which limits the formation of a thick-nitrogen-rich layer.

From these results, a general picture emerges of the nitrating process in metallic alloys. First, the oxygen present in the chamber during deposition is absorbed on the alloy surface following a Langmuir isothermal law. We remark that this behavior was indirectly observed in a previous work.[4] Second, nitrogen diffuses efficiently into the alloy bulk, provided that sufficient active sites are available, i.e., the presence of metallic nitrides such as FeN_x and γ_N is very important to guarantee efficient nitrogen diffusion. On the other hand, the formation of NO_2 surface compounds blocks nitrogen diffusion, i.e., is a limiting diffusion factor. In addition, we found that chromium nitride shows a mild dependence on increasing oxygen partial. Indeed, this behavior possibly indicates a saturation process of chromium nitride formation. In a fine study, Parascandola and co-workers[17] proposed a model to explain nitrogen diffusion in stainless steel. According to these researchers, chromium forms *trap sites* by forming nitrides which inhibit the atom diffusion in the alloy. In the present work, we expand upon these conclusions by identifying the main *active sites* involved in the surfaces process. In light of the present results, the particular role of FeN_x and the γ_N phase on the diffusion efficiency cannot be elucidated. However, these results can serve as guidance for the optimization of implantation processes by promoting the formation of active sites at the surface to improve nitrogen diffusion metal alloys.

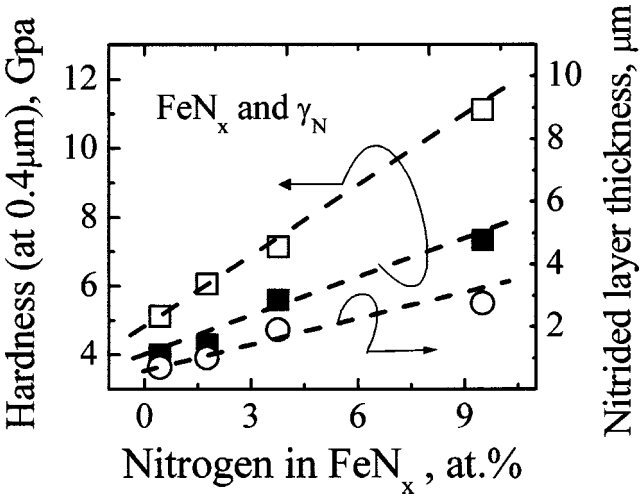

FIG. 4. Filled and empty squares: Hardness (at 0.4 μm depth) of the nitrated layer vs N content in the form of FeN_x compounds of samples implanted for 30 and 60 min, respectively. Open circles: Thickness vs N content in the form of FeN_x for the 30 min implanted samples. The experimental errors are of the order of the symbol size.

In conclusion, the process of oxygen adsorption is explained assuming a Langmuir isothermal law. Three main nitrogen compounds species are formed on the alloy surface: (1) FeN_x and γ_N, (2) CrN_x, and (3) NO_x. The formation of CrN_x seems to depend weakly on oxygen absorption. The presence of oxygen limits the formation of FeN_x and the γ_N phase which has a deleterious effect on the hardness and thickness of the nitrated layer.

This work was partially sponsored by Fapesp. One of the authors (F. A.) is CNPq Fellows and the others (A. S. F. and C.A.F.) are Fapesp Fellows.

[1] M. Hudis, J. Appl. Phys. **44**, 1489 (1973).
[2] A. Szasz, D. J. Fabian, A. Hendry, and Z. Szaszne-Csih, J. Appl. Phys. **66**, 5598 (1989).
[3] S. Parascandola, O. Kruse, and W. Möller, Appl. Phys. Lett. **75**, 1851 (1999).
[4] C. A. Figueroa, D. Wisnivesky, and F. Alvarez, J. Appl. Phys. **92**, 764 (2002).
[5] *Practical Surface Analysis*, 2nd ed., edited by D. Briggs and M. P. Seah (Wiley, New York, 1996), Vol. 1.
[6] P. Hammer, N. M. Victoria, and F. Alvarez, J. Vac. Sci. Technol. A **16**, 2941 (1998).
[7] The mean-free path turns out to be important since the ultimate energy of nitrogen ions depends on this vital parameter. See R. Wei, Surf. Coat. Technol. **83**, 218 (1996).
[8] J. P. B. Biersack and G. L. Haggmark, Nucl. Instrum. Methods **174**, 257 (1980).
[9] W. C. Oliver and G. M. Pharr, J. Mater. Res. **7**, 1564 (1992).
[10] P. W. Atkins, *Physical Chemistry*, 3rd ed. (Oxford University Press, UK, 1986).
[11] E. J. Miola, S. D. de Souza, P. A. P. Nascente, M. Olzon-Dionysio, C. A. Olivieri, and D. Spinelli, Appl. Surf. Sci. **144**, 272 (1999).
[12] P. Marcus and M. E. Bussell, Appl. Surf. Sci. **59**, 7 (1992).
[13] J. P. Riviere, M. Cahoreau, and P. Meheust, J. Appl. Phys. **91**, 6361 (2002).
[14] O. Nishimura, K. Yabe, and M. Iwaki, J. Electron Spectrosc. Relat. Phenom. **49**, 335 (1989).
[15] B. Folkesson, Acta Chem. Scand. **27**, 287 (1973).
[16] See, for instance, *Introduction to Solid State Physics*, edited by C. Kittel, 7th ed. (Wiley, New York, 1996).
[17] S. Parascandola, W. Möller, and D. L. Williamson, Appl. Phys. Lett. **76**, 2194 (2000).